Analyzing the Recognition of Color Exposure and Imagined Color from EEG Signals

1st Alejandro A. Torres-García
Department of Engineering Cybernetics
Norwegian University of Science and Technology (NTNU)
Trondheim, Norway
alejandro.a.t.garcia@ntnu.no

2nd Marta Molinas
Department of Engineering Cybernetics
Norwegian University of Science and Technology (NTNU)
Trondheim, Norway
marta.molinas@ntnu.no

***Abstract*—The most widely used visual brain-computer interfaces (BCIs) are based on flickering stimulators. It remains unclear whether a passive visual stimulator could be used. Colors are an integral part of everyday life. We analyzed the potential use of both imagined colors and color exposure to control BCIs. We present here a comprehensive study of the feasibility of using the recognition of both exposed and imagined colors from the EEG signals recorded in a previous study. This constitutes the first step towards the development of a color-based BCI. We processed and analyzed the EEG signals from seven subjects recorded whilst they were exposed to three colors (red, green and blue) and whilst they imagined the same colors. The outcomes obtained suggest that the simultaneous use of these two tasks would facilitate the effective recognition of both imagined and displayed colors for the control of a BCI. An analysis of each task separately revealed that color exposure provided more information than color imagination for discriminating between the three colors.**

***Index Terms*—classification, imagined colors recognition, exposure color recognition**

I. Introduction

EEG-based brain-computer interfaces (BCIs) are designed to provide individuals with a non-muscular channel for transmitting messages and commands to the external world [1]. Such interfaces were initially designed for use by the disabled, but have since been developed for use by the able-bodied too. The mechanism used for interaction or for generating messages or commands for the BCI is called the neuroparadigm. Motor imaging is the most widely used paradigm for BCI control. However, this approach suffers from being intuitively difficult to achieve. Several studies have investigated alternative approaches based on the use of visual stimuli to control BCIs.

The most common visual paradigms for BCI control (SSVEP and P300) are based on an external flickering stimulator. We aimed to overcome the need for a flickering stimulator by using only EEG responses to primary colors. A color-based recognition system would be easier to use too, because passive stimulators, such as signs indicating the way out and traffic lights, are an integral part of everyday life. The integration of a BCI of this kind into the environment required for home automation would make this system useful for elderly and disabled people. It would provide these individuals with greater autonomy by allowing them to control lights, the virtual keyboard of the computer and music players. It would also make it possible for them to answer the telephone and to ask for assistance in emergencies.

The European Research Consortium for Informatics and Mathematics (ERCIM). 2004, Route des Lucioles. BP93. 06902 Sophia Antipolis, France.

II. Related work

Few studies have focused on the automatic recognition of either displayed or imagined colors from brain signals [2]–[4]. Liu et al. [4] analyzed fNIRS signals, for which time responses remain much less useful for practical applications than those of EEG signals. Yu et al. [3], discussed the use of discrimination between five imagined colors (red, green, blue, yellow and white) recorded for 10 subjects with an Emotiv Epoc headset (14 channels and a sampling frequency of 128 Hz). They claimed that applying a method based on event-related potential (ERP) values (selecting N2, P3 and N4) and artificial neural networks (ANN), yielded a mean accuracy for all subjects of about 65% if channel T7 or F4 was used separately. However, they recorded only ten epochs for each color. Another previous study [2] described the recording of a dataset for three exposed and imagined colors (red, green and blue), and the use of a method based on event-related spectral perturbations (ERSP) and support vector machine (SVM). More epochs (60 epochs per color) were recorded in this study than in the study by Yu [3] and accuracies of 84-97% for exposed colors and 64-76% for imagined colors were achieved, but the three averaged ERSP matrices were calculated from the global information. This meant that the method made use of the data used for training at the testing stage, resulting in an overestimation of method performance. Finally, this method had the drawback of being dependent on a visually supervised stage for artifact removal, decreasing its suitability for practical applications.

The question of the level of performance that can be achieved with the identification of colors from EEG signals, with both good data management and automatic artifact removal, therefore remains unanswered. This comprehensive study using a dataset described elsewhere [2], aimed to provide more evidence concerning the feasibility of using the recog-

nition of exposed and imagined colors from EEG signals as a first step towards the development of a color-based BCI.

We performed three sets of experiments. In the first, we assessed the feasibility of simultaneously recognizing all the exposed and imagined colors. In the second, we investigated whether a machine learning algorithm could suggest differences or similarities between exposed and imagined colors. In the third, we separately analyzed the feasibility of recognizing the three imagined colors and the three exposed colors. This last experiment was designed to determine which approach would be most suitable for practical applications in BCI control.

III. Dataset

In this work, we processed and analyzed the dataset recorded in a previous study [2], consisting of the EEG signals recorded during both exposure to colors and the imagination of colors. The study participants were exposed to and asked to imagine the colors red, green, and blue. Signals were obtained from the seven subjects by recording on a four-channel g.Tec MOBIlab device with a sampling frequency of 256 Hz. In accordance with the 10-20 international system, the channel names were P1, P2, O1, and O2. The recording protocol consisted of the random presentation of any exposed or imagined color for 3 seconds per epoch. After the presentation of each epoch of imagined or exposed color, a gray screen was displayed for 3 seconds. Subjects were asked to keep their eyes closed during the imagination of colors. At the end of the recording period, the dataset for each subject consisted of 60 epochs for each exposed and imagined color. At the end of the study, we had six classes available and 360 epochs per subject.

IV. Method

The proposed method consists of the following stages: preprocessing, feature extraction and classification. Figure 1 illustrates the method stages and provides a global overview of the specific techniques analyzed. The preprocessing and feature extraction stages calculate feature vectors for each epoch of EEG signals (from all channels) recorded during the imagination or exposure of colors. The arrangement of the dataset depended on the aims of the experiment concerned. These feature vectors were then used in the classification stage, for the assessment of performance, using four classifiers after the application of 10-fold cross-validation. Specific details are provided below for each stage of the method.

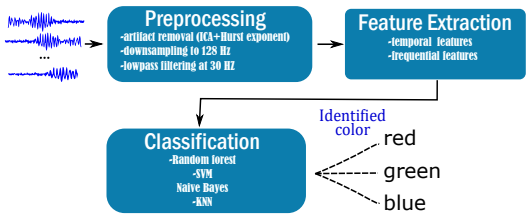

Fig. 1. Method used for the classification of EEG signals recorded during exposure to colors and the imagination of colors

A. Preprocessing

At this stage, an automatic method (described in [5]) was used to remove artifacts. This method was based on independent component analysis and assessment of the components obtained with the Hurst exponent. These method discards components with Hurst exponents in the range 0.58-0.69 because such components are more likely to be related to eye blinks and heartbeats [5]. The remaining components are then mixed again to reconstruct the EEG signals. All epochs with no useful components are automatically removed from the dataset. It should be stressed that, in this work, we set the number of independent components to be calculated as equal to the number of available electrodes. Later on, the signals were downsampled to 128 Hz. They were then low-pass filtered at 30 Hz, to eliminate most of the artifact-related activity.

B. Feature extraction

Given the relevance of considering both the non-stationary nature of EEG signals and temporal changes in the features (see [6]), we computed a set of temporal and frequency features from each epoch of color exposure and imagination. For the temporal features, we calculated, for each epoch and channel, the mean, median, standard deviation, variance, maximum, minimum, sum, difference and sum of the maximum and minimum, kurtosis, skewness, entropy, zero-crossing rate and autoregressive coefficients (6th order).

By contrast, the frequency features were computed after the application of discrete wavelet transform (DWT), with a biorthogonal 2.2 as the mother wavelet and four levels of decomposition. We chose this number of levels to capture the activity of brain rhythms in different ways. Table I shows the decomposition levels and their corresponding frequency ranges and brain rhythms. Following the low-pass filtering of signals at 30 Hz, the D1 coefficients were rejected for subsequent analyses.

TABLE I
Description of the levels of DWT decomposition, their frequency ranges and related brain rhythms

Level	Freq. range	Brain rhythm
D1	32-64	*gamma*
D2	16-32	*beta* (16-30 Hz.), and *gamma* (30-32 Hz.)
D3	8-16	*alpha* (8-12 Hz.), and *beta* (12-16 Hz.)
D4	4-8	*theta*
A4	0-4	*delta*

For each remaining wavelet decomposition level (D2-D4 and A4), we calculated the teager (TWE), instantaneous (IWE), relative (RWE) [7] and hierarchical (HWE) energies, along with the following statistical values: the mean, median, standard deviation, variance, ratio of the means in adjacent sub-bands, maximum, minimum, sum, difference and sum of the maximum and minimum, kurtosis, and skewness. Finally, we concatenated all the features from each epoch in the following order P1, P2, O1, and O2.

TWE and HWE are much less well known in BCI research than RWE, as they were first applied to automatic speech recognition (ASR) [8], making it possible to capture differences not considered by IWE. IWE captures the mean amplitude of the signal, whereas TWE helps to reduce the effect of additive noise by considering the neighboring values of an element of the signal before computing the corresponding energy. Finally, HWE [9] was proposed for the analysis of the central energy of a given analysis window, using the same number of coefficients in every band. Below, we show the corresponding formulas for each j-th decomposition level.

IWE_j is computed as follows,

$$IWE_j = \log_{10}\left(\frac{1}{N_j}\sum_{r=1}^{N_j}(w_j(r))^2\right), \tag{1}$$

where w_j are the wavelet coefficients at the j-th level of decomposition , and N_j is the number of samples at the j-th level of decomposition.

TWE_j can be computed as follows,

$$TWE_j = \log_{10}\left(\frac{1}{N_j}\sum_{r=1}^{N_j-1}|(w_j(r))^2 - w_j(r-1) * w_j(r+1)|\right), \tag{2}$$

where w_j are the wavelet coefficients at the j-th level of decomposition, and N_j is the number of samples at the j-th level of decomposition.

HWE can be computed as follows,

$$HWE_j = \log_{10}\left(\frac{1}{N_J}\sum_{r=(N_j-N_J)/2}^{(N_j+N_J)/2}(w_j(r))^2\right), \tag{3}$$

where w_j are the wavelet coefficients at this level, N_j is the number of samples at this level, and N_J is the number of samples at the last level of decomposition.

C. Classification

Classification covers any context in which a decision or forecast is made on the basis of available historical data (see section III in our case). Specifically, a supervised classification problem has a database of the form [10]:

$$D = \{\langle x_1, y_1\rangle, \langle x_2, y_2\rangle, \cdots, \langle x_m, y_m\rangle\} = \langle X, Y\rangle \tag{4}$$

where the values $x_i \in X$ are typically multidimensional vectors (here, instances or epochs) of the form: $x_i = \{z_1, z_2, \cdots, z_n\}$ the elements of which can take continues or discrete values. These components are called attributes (or features). In our experiment, these values are the frequential and temporal features computed for each epoch. The goal is to infer a function (or relationship) f mapping the elements of X to Y, $f : X \to Y$.

The values of Y are contained in a finite set of classes $C = \{C_1, ..., C_k\}$ that characterize the given data (here 2, 3 or 6 classes, depending on the experiment analyzed). The models learned from training data are then evaluated with a different set of tests to determine whether they can be generalized to new cases [11]. Finally, cross-fold validation is performed, in which the original data are partitioned into k subsamples. The model is then trained on k-1 subsamples, the remaining subsample being used to test the model. Each subsample is used separately to test the model and an estimated generalization error is then calculated.

Despite the deep learning's boom in many machine learning applications, most of these algorithms usually do not get outstanding performances when small datasets are available such as it commonly happens in BCIs [12]. Accordingly, we trained and tested the following four classifiers: support vector machine (SVM), random forests (RFs), naive Bayes (NB) and K-nearest neighbors (KNN). Each of these classifiers differ in nature. Random forests are a fast ensemble of decision trees, Naive Bayes is based on Bayes theorem, SVM is based on the kernel trick to find the hyperplane maximizing the separation between classes and KNN is based on the majority class in a set of k neighbors. Specifically, we used 50 trees for RF and k=3 for KNN, the remaining hyperparameters were obtained with the default values of the Weka toolbox [13]. Subsequent experiments were performed on different arrangements of the dataset, and performance was assessed by 10-fold cross-validation. The specific details of each classifier are presented below.

1) SVM: SVM uses a discriminating hyperplane to identify classes. The selected hyperplane is that which maximizes the margins for the SVM classifier, that is, the distance between the closest training points, with the aim of increasing generalization capabilities [14], [15]. SVM uses a C regularization parameter that can accommodate outliers and is robust to errors in the training set, which are common for EEG signals.

We used a linear SVM, implying the use of linear decision boundaries for classification. However, non-linear decision boundaries can be created with the kernel trick. This involves the implicit assignment of data to another space (usually of a higher dimension) by a kernel function. Some of the most widely used alternative kernels are the radial base, Gaussian, polynomial and sigmoid functions. In multiclass problems, such as some of the experiments in this work, SVMs are applied by the so-called "OVR" (one versus the rest) strategy, which involves separating each class from all the others [16]. Such an approach is suitable for use in the context of the recognition of exposed and imagined colors. SVMs have many advantages, including good generalization properties, and insensitivity to over-training and dimensionality [14], [15].

2) NB: NB is based on the determined probabilities of the data. New objects can be assigned to classes with various degrees of probability [11]. NB assumes that the attributes are independent, (i. e., that the effect of an attribute on a specific class does not depend on the values of the remaining attributes (variables or features)).

NB is based on Bayes Theorem:

$$P(h|D) = \frac{P(D|h)\cdot P(h)}{P(D)}, \tag{5}$$

where $P(h)$ is the probability *a priori* of the hypothesis h, $P(D)$ is the probability *a priori* of the training data D,

$P(h|D)$ is the probability of h given D, and $P(D|h)$ is the probability of D given h. In general, the most likely hypothesis for the given training data is calculated to obtain the most likely hypothesis *a posteriori* h_{MAP}, which is computed as follows,

$$\begin{aligned} h_{MAP} &= \underset{h \in H}{arg\ max}\ P(h|D) \\ &= \underset{h \in H}{arg\ max}\ \frac{P(D|h) \cdot P(h)}{P(D)} \\ &= \underset{h \in H}{arg\ max}\ P(D|h) \cdot P(h) \end{aligned} \tag{6}$$

If we assume that $P(h_i) = P(h_j)$, then further simplification is possible, by selecting the hypothesis with the maximum likelihood, that is:

$$h_{ML} = \underset{h_i \in H}{arg\ max}\ P(D|h_i) \tag{7}$$

NB can then be combined with a decision rule for data classification. A common rule used for this purpose is selection of the most likely hypothesis for an unlabeled vector, via MAP or ML methods.

3) Random forests (RF): RFs are combinations of predictor trees such that each tree depends on the values of a random vector sampled independently and with the same distribution for all trees in the forest. Each tree casts a single vote for the most popular class for a given instance x. The output of RF is then obtained by a sort of "majority voting" system. The trees are constructed with algorithm 1. The generalization error over forests almost certainly converges to a limit as the number of trees in the forest increases [17].

Algorithm 1 Random Forest

Require: IDT (a decision tree), T (the number of iterations), S (the training set), μ (the size of the subsample), N (the number of attributes at each node)
Ensure: M_t; $t = 1, \ldots, T$
for $t \leftarrow 1$ to T **do**
  $S_t \leftarrow$ a sample with μ instances from S allowing replacement
  Build the classifier M_t using $IDT(N)$ on S_t.
end for

In algorithm 1, IDT represents a decision tree with the following modifications: the decision tree is not pruned, and at each node, instead of selecting the best division from all the attributes, the inducer randomly samples N attributes and selects the best division from them. Finally, the key advantages of the random forest approach are: its speed and the ease with which it can handle a large number of input attributes [18].

4) K nearest neighbors (KNN): KNN is based on the comparison of the object to be classified with all objects stored in the dataset. The class of the unknown object x_j is assigned by analyzing the known classes of the k examples (neighbors) most similar to the object in the dataset. The object is assigned to the majority class among the neighbors [10].

The key to this classifier is the definition of the nearest neighbors $\mathbf{x}_1^N, \ldots, \mathbf{x}_k^N$ to a given instance (example or epoch) $\mathbf{x}_j$. This is achieved by measuring the distance between the object to be classified and all the elements in the dataset. The k instances with the smaller distances (generally Euclidean distances) to the instance concerned are considered to be its nearest neighbors. Finally, the number of neighbors k selected is typically odd rather than even (K=3 in this work) to avoid draws in votes for the output class [10].

V. Experiment and results

A. Recognition of all the exposed and imagined colors

In this experiment, we investigated whether a machine learning algorithm could discriminate between all the exposed and imagined colors. In this case, there were six available classes (red, green and blue, along with the epochs recorded during the imagination of these colors). Table II shows the accuracy (expressed as a percentage) and standard deviations (SDs) for all four classifiers after 10-fold cross-validation for all subjects. For all classifiers, the mean accuracy for all subjects and for each subject individually was above expectations based on chance alone for the six classes (16%). This suggests that there was a difference between each of the exposed and imagined colors.

TABLE II
Percent accuracy and SDs obtained for the classifiers for the recognition of all the imagined and exposed colors (6 classes)

subj	SVM		RF		NB		KNN	
	acc	std	acc	std	acc	std	acc	std
S1	27.64	8.17	30.12	7.8	26.23	5.31	27.4	6.89
S2	30.72	7.72	27.65	3.54	20.96	6.15	26.84	5.77
S3	33.89	9.15	37.78	5.27	37.78	8.2	33.06	5.92
S4	25.83	6.29	27.78	3.93	26.39	6.84	20.56	5.43
S5	29.44	6.44	30	4.1	28.61	6.81	25.56	8.57
S6	30	5.97	27.22	7.5	28.61	4.91	27.22	5.83
S7	33.61	7.91	32.78	9.15	29.44	8.2	32.22	6.31
Avg	30.16	7.38	30.48	5.9	28.29	6.63	27.55	6.39

The imagined colors were recorded with the eyes closed. In the next experiment, we eliminated the impact of the main rhythm related to this activity by removing the alpha band, which has been reported to be the most relevant difference between open and closed eyes [19]. We applied a stop-band filter (4-12 Hz) to the six classes before the feature extraction stage. The outcomes can be seen in Table III. Despite the decrease in mean performance for the classifiers, performance remained above expectations based on chance alone for all six classes.

B. Recognition of exposed and imagined colors

In this experiment, we investigated whether a machine learning algorithm could use differences or similarities between imagined and actual colors to distinguish between them (i.e, differences result in high levels of accuracy and similarities results in low levels of accuracy). In this case, we ran a binary classification scheme. For each subject, all the epochs

TABLE III
PERCENT ACCURACY AND SDS OBTAINED FOR THE CLASSIFIERS FOR THE RECOGNITION OF ALL THE IMAGINED AND EXPOSED COLORS (6 CLASSES WITH REMOVAL OF THE ALPHA BAND)

subj	SVM		RF		NB		KNN	
	acc	std	acc	std	acc	std	acc	std
S1	23.44	8.93	28.18	5.94	22.35	5.9	20.13	3.52
S2	27.1	5.09	24.33	10.39	19.79	7.15	20.42	5.71
S3	28.89	7.2	30.83	8.53	36.39	8.43	28.33	5.68
S4	22.22	2.62	20.56	6.7	22.78	7.03	16.67	5.71
S5	32.22	8.9	25.83	8.98	21.39	5.56	25	6.93
S6	20.83	5.44	19.72	5.31	18.61	6.15	22.5	6.47
S7	28.06	7.11	26.94	7.64	24.44	7.61	23.33	7.2
Avg	26.11	6.47	25.2	7.64	23.68	6.83	22.34	5.89

recorded during either exposure to colors or the imagination of colors were managed as single classes. Table IV shows the percent accuracy and standard deviations for all four classifiers after 10-fold cross-validation for all subjects. For all four classifiers, the mean accuracy for all subjects was above chance expectations for two classes, suggesting a difference between exposed and imagined colors.

TABLE IV
PERCENT ACCURACY AND STANDARD DEVIATIONS OBTAINED FOR THE CLASSIFIERS FOR THE RECOGNITION OF EXPOSED AND IMAGINED COLORS

subj	SVM		RF		NB		KNN	
	acc	std	acc	std	acc	std	acc	std
S1	87.11	6.71	86.55	7.9	74.56	8.04	77.9	8.74
S2	82.66	6.06	85.52	7.57	64.79	7.1	78.81	7.49
S3	97.22	1.85	98.33	2.68	98.33	2.68	96.94	3.33
S4	75	7.52	76.39	9	59.17	5.72	67.5	7.18
S5	75.83	5.56	77.5	5.92	72.5	5.15	76.39	6.84
S6	88.06	4.35	89.72	3.72	78.61	6.68	85.28	5.56
S7	96.39	2.64	98.06	2.64	96.39	2.94	97.22	2.93
Avg	86.04	4.96	87.44	5.63	77.76	5.47	82.86	6.01

We assessed the impact of the eyes being closed during the imagination tasks on the performances obtained in Table IV, by applying a stop-band filter (4-12 Hz) to the signals before the feature extraction stage. Table V shows the performance achieved when this filter was applied to both classes. A better performance was achieved when the alpha rhythm was retained, but all mean performances in Table V were nevertheless above chance expectations for two classes.

C. Separate recognition of exposed and imagined colors

In these experiments, we separately analyzed the epochs for the three classes recorded during exposure to colors and the imagination of colors, to assess the feasibility of color recognition in both situations. For exposed colors, Table VI shows the percent accuracy and standard deviations for all the classifiers and for each subject analyzed. The highest mean accuracy was obtained with random forest (37.64%). For some subjects, accuracy was considerably higher than chance expectations for three classes (33%). For example, S3 and S5 achieved accuracies of 45.56% and 43.33, respectively. These individual performances were also consistent with those for the other classifiers. Accuracy for SVM was highest for S5, and accuracy for NB was highest for S3.

TABLE V
PERCENT ACC AND SDS GOT FOR THE CLASSIFIERS FOR THE RECOGNITION OF EXPOSED AND IMAGINED COLORS (WITH REMOVAL OF THE ALPHA BAND)

subj	SVM		RF		NB		KNN	
	acc	std	acc	std	acc	std	acc	std
S1	82.13	4.13	81.28	5.35	71.48	7.95	71.75	9.45
S2	78.18	6.25	77.36	6.81	56.97	5.88	62.56	10.62
S3	97.5	2.05	97.78	2.55	96.11	1.94	97.78	1.17
S4	65.28	7.88	71.11	6.31	56.67	3.75	57.78	8.36
S5	78.61	5.86	78.89	6.7	59.44	7.77	67.78	6.83
S6	75	3.93	77.5	4.98	64.72	6.15	66.67	6.28
S7	92.5	4.91	93.33	4.18	80.28	6.47	81.67	5.27
Avg	81.31	5	82.46	5.27	69.38	5.7	72.28	6.85

TABLE VI
PERCENT ACCURACY AND STANDARD DEVIATIONS OBTAINED FOR THE CLASSIFIERS FOR RECOGNITION OF THE THREE EXPOSED COLORS

subj	SVM		RF		NB		KNN	
	acc	std	acc	std	acc	std	acc	std
S1	35.36	9.7	35.52	11.1	32.58	6.9	32.52	10
S2	32.45	14.4	38.5	10.1	32.35	11.5	26.21	7.3
S3	38.33	8.5	45.56	8.2	44.44	9.1	32.78	9.2
S4	36.11	15.3	33.33	9.1	42.22	18.7	33.33	9.8
S5	41.11	15.1	43.33	7.8	36.67	14.9	31.11	12.1
S6	28.33	6.1	27.78	12	36.11	14.2	34.44	9
S7	41.11	9.5	39.44	9.2	31.11	10.9	32.78	12.7
Avg	36.11	11.2	37.64	9.6	36.5	12.3	31.88	10

By contrast, Table VII shows the percent accuracy and standard deviations for the analysis of the three imagined colors. The highest mean accuracy was achieved with SVM (35.9%). However, the highest absolute value for accuracy (39.44%) was that for S3 and S4 using RF. Regardless of the classifier used, accuracy was close to chance expectations for three classes (33%). Furthermore, taking into account the standard deviation for the best subjects, their performances were no better than would have been expected by chance. These results suggest that it is more difficult to control devices using only imagined colors.

TABLE VII
PERCENT ACCURACY AND SDS OBTAINED FOR THE CLASSIFIERS FOR RECOGNITION OF THE THREE IMAGINED COLORS

subj	SVM		RF		NB		KNN	
	acc	std	acc	std	acc	std	acc	std
S1	31.11	8.8	34.44	11.7	33.89	14.9	30.56	11.5
S2	36.86	10.2	29.71	10.9	35.82	10.5	30.16	10.8
S3	36.11	9.9	39.44	15.4	33.89	11.8	31.67	13.1
S4	33.89	12.4	39.44	9.2	29.44	9.5	34.44	6.3
S5	37.78	13.3	30	12.6	37.22	7.9	37.78	6.8
S6	37.78	10.4	30.56	10.2	33.89	8.5	35	11.7
S7	37.78	9.7	33.33	7.9	36.67	9.9	37.22	7.9
Avg	35.9	10.7	33.85	11.1	34.4	10.4	33.83	9.7

We also assessed the impact of removing the alpha band from the epochs of the three imagined colors before the feature

extraction stage. This activity was expected to be common to these three classes. Table VIII shows the performances obtained with this filtering. These results suggest that this brain rhythm does not have a major impact on the performance of the classifiers.

TABLE VIII
PERCENT ACCURACY AND SDS OBTAINED FOR THE CLASSIFIERS FOR THE RECOGNITION OF THE THREE IMAGINED COLORS (WITH REMOVAL OF ALPHA RHYTHMS)

subj	SVM		RF		NB		KNN	
	acc	std	acc	std	acc	std	acc	std
S1	35	15.3	36.11	8.8	37.78	17.5	28.33	7.6
S2	43.53	10.2	36.76	13.8	35.82	16.4	36.21	13.3
S3	25.56	6.5	31.67	10.5	38.89	10.5	32.22	13.8
S4	33.33	9.4	33.89	13.0	30.56	8.0	25.56	10.9
S5	27.78	10.1	36.11	11.5	34.44	9.0	35.56	12.3
S6	32.78	17.9	33.89	10.0	32.78	7.6	36.67	10.5
S7	30.56	4.7	26.67	6.3	32.78	8.5	25	9.2
Avg	32.65	10.6	33.59	10.5	34.72	11.1	31.36	11.1

VI. CONCLUSIONS

We present here a comprehensive study of the feasibility of recognizing both exposed and imagined colors from EEG signals. We analyzed a dataset obtained by exposing subjects to three colors (red, green and blue) and asking them to imagine these same three colors. We designed a scheme including an automatic artifact removal method, the extraction of both temporal and frequency features, and the assessment of a set of four classifiers of different natures. Besides, we had a special care of the use of the available data to avoid overestimated outcomes. We also performed additional validations to ensure that the outcomes obtained were not related to the main difference between exposure to colors and the imagination of colors (eyes open and closed, respectively), by removing the alpha band before the feature extraction stage in the experiments concerned.

The outcomes got for all exposed and imagined colors simultaneously suggested that the recognition of these six classes was feasible. This performance was maintained even if alpha rhythms were removed from all the classes. We then designed a binary experiment assessing the ability to distinguish between exposed and imagined colors. All the classifiers had percent accuracy values above chance expectations (even after the removal of alpha rhythms). This suggests a difference between the EEG signals recorded during exposure to colors and those recorded during the imagination of colors. This may explain the good performance in the first experiment. Finally, we analyzed the separate recognition of imagined and exposed colors. The outcomes suggest that exposure to colors is more suitable than the imagination of colors for the development of color-based BCIs, consistent with the outcomes reported in a previous study [2] (despite their overestimation). However, the performance was subject-dependent for color exposure. These outcomes could potentially be improved by applying a feature selection stage to analyze fewer features in each epoch.

Despite the promising outcomes got here, particularly for discrimination between exposure to colors and the imagination of colors, further studies are required to improve our understanding of this neuroparadigm and its potential use for controlling BCIs. We will focus, in particular, on increasing the numbers of subjects and epochs to determine whether the performance of this method could be improved or, at least, maintained. Furthermore, the recording of this new dataset will keep in mind to get a suitable amount of instances for testing deep learning algorithms too.

ACKNOWLEDGMENTS

We would like to thank Prof. S. Rasheed for providing us with his dataset. We also thank the ERCIM for supporting this research with a fellowship.

REFERENCES

[1] J. R. Wolpaw, N. Birbaumer, D. J. McFarland, G. Pfurtscheller, and T. M. Vaughan, "Brain–computer interfaces for communication and control," *Clinical neurophysiology*, vol. 113, no. 6, pp. 767–791, 2002.

[2] S. Rasheed, *Recognition of primary colours in electroencephalograph signals using support vector machines*. PhD thesis, Università degli Studi di Milano, 2011.

[3] J.-H. Yu and K.-B. Sim, "Classification of color imagination using Emotiv EPOC and event-related potential in electroencephalogram," *Optik*, vol. 127, no. 20, pp. 9711–9718, 2016.

[4] X. Liu and K.-S. Hong, "Detection of primary RGB colors projected on a screen using fNIRS," *Journal of Innovative Optical Health Sciences*, vol. 10, no. 03, p. 1750006, 2017.

[5] S. Vorobyov and A. Cichocki, "Blind noise reduction for multisensory signals using ICA and subspace filtering, with application to EEG analysis," *Biological Cybernetics*, vol. 86, no. 4, pp. 293–303, 2002.

[6] F. Lotte, M. Congedo, A. Lcuyer, F. Lamarche, and B. Arnald, "A review of classication algorithms for EEG-based brain-computer interfaces," *Journal of Neural Engineering*, vol. 4, pp. r1–r13, 2007.

[7] L. Guo, D. Rivero, J. Seoane, and A. Pazos, "Classification of EEG signals using relative wavelet energy and artificial neural networks," in *Proceedings of the first ACM/SIGEVO Summit on Genetic and Evolutionary Computation*, pp. 177–184, ACM, 2009.

[8] E. Didiot, I. Illina, D. Fohr, and O. Mella, "A wavelet-based parameterization for speech/music discrimination," *Computer Speech & Language*, vol. 24, no. 2, pp. 341–357, 2010.

[9] D. Kryze, L. Rigazio, T. Applebaum, and J.-C. Junqua, "A new noise-robust subband front-end and its comparison to PLP," in *Workshop on Automatic Speech Recognition and Understanding (ASRU*, IEEE, 1999.

[10] D. Michie, D. Spiegelhalter, and C. Taylor, *Machine Learning, Neural and Statistical Classification*. Prentice Hall, 1994.

[11] R. Jensen and Q. Shen, *Computational intelligence and feature selection: rough and fuzzy approaches*. IEEE Press, 2008.

[12] F. Lotte, L. Bougrain, A. Cichocki, M. Clerc, M. Congedo, A. Rakotomamonjy, and F. Yger, "A review of classification algorithms for EEG-based brain–computer interfaces: a 10 year update," *Journal of neural engineering*, vol. 15, no. 3, p. 031005, 2018.

[13] I. H. Witten, E. Frank, M. A. Hall, and C. J. Pal, *Data Mining: Practical machine learning tools and techniques*. Morgan Kaufmann, 2016.

[14] C. Burges, "A tutorial on support vector machines for pattern recognition," *Data mining and knowledge discovery*, vol. 2, no. 2, pp. 121–167, 1998.

[15] K. Bennett and C. Campbell, "Support vector machines: hype or hallelujah?," *ACM SIGKDD Explorations Newsletter*, vol. 2, no. 2, pp. 1–13, 2000.

[16] A. Schlögl, F. Lee, H. Bischof, and G. Pfurtscheller, "Characterization of four-class motor imagery EEG data for the BCI-competition 2005," *Journal of neural engineering*, vol. 2, p. L14, 2005.

[17] L. Breiman, "Random forests," *Machine learning*, vol. 45, no. 1, pp. 5–32, 2001.

[18] L. Rokach, *Pattern Classification Using Ensemble Methods*. World Scientific, 2009.

[19] R. J. Barry, A. R. Clarke, S. J. Johnstone, C. A. Magee, and J. A. Rushby, "EEG differences between eyes-closed and eyes-open resting conditions," *Clinical Neurophysiology*, vol. 118, no. 12, pp. 2765–2773, 2007.